Nuclear Instruments and Methods in Physics Research B 292 (2012) 11–17

Contents lists available at SciVerse ScienceDirect

Nuclear Instruments and Methods in Physics Research B

journal homepage: www.elsevier.com/locate/nimb

Sputtering and surface topography modification of bismuth thin films under swift $^{84}Kr^{15+}$ ion irradiation

S. Mammeri [a], S. Ouichaoui [b,*], H. Ammi [a], C.A. Pineda-Vargas [c,d], A. Dib [a], M. Msimanga [c]

[a] Centre de Recherche Nucléaire d'Alger, CRNA, B.P. 399, 02 Bd. Frantz Fanon, Alger-Gare, Algiers, Algeria
[b] Université des Sciences et de la Technologie H. Boumediene (USTHB), Faculté de Physique, Laboratoire SNIRM, B.P. 32, El-Alia, 16111 Bab Ezzouar, Algiers, Algeria
[c] iThemba LABS, National Research Foundation, P.O. Box 722, Somerset West 7129, South Africa
[d] Faculty of Health and Wellness Sciences, CPUT, P.O. Box 1906, Bellville 7535, South Africa

ARTICLE INFO

Article history:
Received 16 August 2011
Received in revised form 16 July 2012
Available online 9 October 2012

Keywords:
SHI irradiation
Electronic stopping
Surface sputtering
Rutherford backscattering spectrometry (RBS)
Atomic force microscopy (AFM)
X-rays diffraction (XRD)

ABSTRACT

The sputtering and surface topography modification of bismuth thin films deposited onto Si substrates and irradiated by 27.5 MeV $^{84}Kr^{15+}$ ions over the fluence range 10^{12}–10^{14} cm^{-2} have been studied using three complementary techniques: Rutherford backscattering spectrometry (RBS), atomic force microscopy (AFM) and X-ray diffraction (XRD). The RBS analysis reveals a linear reduction of the initial thickness of the irradiated bismuth samples by ~4% up to 7% with increasing ion fluence corresponding to a mean sputtering yield of $\sim 2.9 \times 10^2$ at/ion. Besides, significant sample surface topography changes occur upon ion irradiation consisting in grain growth and surface roughening clearly pointed out by performed AFM and XRD analyses. Moreover, a close correlation is observed between the variations versus ion fluence of the measured sputtering yield and the determined Bi surface grain size and compressive strain. These moderate Bi surface effects are similar to those pointed out previously for thin films irradiated by MeV heavy ions. They can be mainly caused by inelastic electronic collision mechanisms taking place within the Bi material electronic stopping power regime below the threshold for latent track formation.

1. Introduction

While traversing solid materials, energetic ions may undergo large energy losses and are consequently slowed down either via elastic nuclear collisions (for low energy incident ions in the keV range) or inelastic electronic collisions (i.e., excitations and ionizations of target atoms for high energy incident ions in the MeV–GeV ranges). Both two types of collisions give rise to damage and structure modifications in the solid often accompanied by the erosion of the target material surface (or sputtering). In the case of swift heavy ions (SHI), typically moving on straight paths in the target, material damage ranging from point defects up to phase transitions involving extended ion tracks of nearly cylindrical shapes are produced in insulators. In contrast, in pure metals the deposited electronic excitation energy is rapidly dissipated through the lattice before any damage can be created. From a theoretical point of view, unlike the processes of the initial kinetic energy transfer to target atoms, the mechanisms behind the conversion of the deposited electronic excitation energy into heat of the material lattice, then to complex atomic motions (atomic displacements, ion/atom collision cascades) inducing various types of material damage are yet far from being well elucidated. The nuclear sputtering of the material, induced by keV ions and presumably due mainly to elastic collision cascades of recoil target atoms, has been intensively investigated experimentally, by theory and by modeling during several decades [1–3]. The electronic sputtering, induced by SHI irradiation and expected to be caused by inelastic collisions, has also been studied principally for insulators and for some metallic targets [4–6] (and references therein). More than for other materials, in the case of semi-metallic (polycrystalline) targets having specific properties like bismuth (Bi), however, SHI irradiation-induced effects and underlying mechanisms are still much less investigated and well understood [7–10]. Target material damage induced by strong electronic energy losses under SHI irradiation has been evidenced experimentally in in-situ electrical resistance measurements for bulk Bi [8–10]. Two main distinct theoretical models of the electronic excitation energy transfer to the lattice atoms are usually invoked for describing the SHI irradiation-induced damage, which are: (i) Coulomb explosion [11] and (ii) thermal spikes mechanism [9], beside molecular dynamic numerical simulations [12]. According to the former model, valid at least at the initial stage of the material damage, a lattice zone around the incident ion central path is partially or fully stripped of electrons with the produced ions or bare nuclei being violently ejected radially outward under the action of strong electric forces. Then, they

* Corresponding author. Tel.: +213 7 74 03 77 52; fax: +213 21 24 73 44.
E-mail addresses: souchaoui@gmail.com, souichaoui@usthb.dz (S. Ouichaoui).

0168-583X/$ - see front matter © 2012 Elsevier B.V. All rights reserved.
http://dx.doi.org/10.1016/j.nimb.2012.09.033

can be rapidly re-screened by initially freed target atomic electrons. In the second main electronic energy transfer model, excited electrons heat the lattice via electron–phonon coupling, which leads to a localized, transcient and highly disordered zone at high temperature, likely generated by nonlinear ion/atom collision cascades. Especially the latter so-called *thermal spikes* model was successfully used to account for SHI irradiation-induced surface damage such as the creation of latent tracks above a threshold value of the material electronic stopping power (~24 keV/nm for Bi, see reference [8]) leading to the amorphization of initially crystalline materials. For polycrystalline targets, like deposited Bi thin films, the mechanisms behind the sputtering process within the electronic stopping power regime should then operate differently regarding the crucial dependence of SHI irradiation-induced effects on target properties like the sample thickness and the grown grain size [4,13–16]. Obviously, the magnitude of the damage induced in the material also depends on the intrinsic properties of the latter (chemical bonding, electrical conductivity, aggregation state) and on SHI irradiation conditions like the incident ion energy and fluence. Therefore, materials of different natures are expected to be differently effected under the same ion irradiation conditions.

In the current paper, we report on a careful experimental investigation of the sputtering and surface topography modifications suffered by Bi thin films deposited onto Si substrates under normal impacts of 27.5 MeV $^{84}Kr^{15+}$ ions. Beside the main objective of performing quantitative measurements of the induced surface effects in Bi, we attempted to understand the experimental observations by highlighting, following other groups, the above ion-surface interaction mechanisms that are still being debated. For comparison to previous measurements and interpreting the observed (moderate) SHI irradiation effects, we will also refer to our recent works on similar Bi thin films irradiated by keV Ar^+ ions [17,18]. In those experiments, the sputtering yield data and other observed Bi surface effects were satisfactorily interpreted by primarily invoking interaction mechanisms supporting the generation of linear elastic collision cascades [2,19]. In the current study, evaluating Bi electronic and nuclear stopping powers (S_e and S_n) for 27.5 MeV Kr incident ions and the mean projected range (R_p) of the latter in Bi using the SRIM-2010 computer code [20], one finds values of ~8.08 keV/nm, 0.18 keV/nm and 5.35 µm, respectively. Thus, one has $S_e >> S_n$ and $R_p >> t \sim 0.3$ µm (the mean thickness of the Bi samples used in this experiment). Therefore, one expects all incident ^{84}Kr ions striking the Bi target film to fully cross the latter, stopping far away outside it. Notice that the estimated Bi stopping power is only of 1/3 of the threshold value for which one could assume strong SHI irradiation-induced surface damage to occur, like latent tracks or amorphization [8]. In these conditions, the observed modifications suffered by the Bi film surface upon SHI irradiation are moderate and likely essentially caused by electronic collision interaction mechanisms (ion/atom recoils and displacements). However, although one expects, in first sight, these processes to be the main cause behind the observed high Bi sputtering yield and other irradiation-induced surface effects, elastic nuclear collision mechanisms may also play a non negligible role in this respect.

In the following we, first, succinctly report (in Section 2) on the general experimental method, set up and techniques used described in more detail elsewhere [17,18]. Then, we present and discuss (in Section 3) the obtained experimental results before giving a summary and concluding (in Section 4).

2. Experimental

High purity (99.99%) thin Bi films were deposited by high vacuum evaporation (target chamber pressure of $\sim 8 \times 10^{-7}$ mbar) onto well cleaned and polished Si (100) substrates at room temperature using an electron beam. The evaporation rate during the film deposition process was kept between 2 and 4 Å/s for obtaining smooth sample surfaces [21]. The target sample thicknesses were estimated, first, by means of an *Inficon* monitor deposition apparatus connected to the evaporator displaying the deposited Bi layer with a relative uncertainty of ±1.5%; then, they were more quantitatively determined by RBS spectrometry. About 300 nm-thick Bi samples were used in these experiments. They were placed inside a scattering chamber under high vacuum (under mean pressure of $\sim 2 \times 10^{-6}$ mbar) and irradiated by 27.5 MeV $^{84}Kr^q$ ions at equilibrium charge state, q = +15, delivered by the 2nd solid-pole injector cyclotron (SPC2) of the iThemba Labs in Somerset West, South Africa. The irradiations were performed uniformly over each scanned Bi sample surface at room temperature with varying the incident ion fluence in the range 8.9×10^{12}–1.35×10^{14} cm^{-2} using a beam spot of rectangular shape (2.0 ± 0.1 cm × 1.5 ± 0.1 cm) that was incident normally to the Bi film surface. During SHI irradiations, the beam current intensity was maintained at a low mean value of ~107 nA (mean current density of $\sim 1.5 \times 10^{10}$ ions/cm^2/s) in order to avoid the excessive heating or melting of the samples [4]. Then, in a subsequent step, the irradiated samples were analyzed in thickness by RBS spectroscopy for evaluating the sputter yields (see Section 3 and Ref. [17]). The RBS analyses were conducted using a 2-MeV $^4He^+$ ion beam delivered by the 5.5-MV Van de Graaff accelerator of the iThemba Labs with mean current intensity of ~40 nA. Backscattered alpha particles were detected by means of a well collimated surface barrier Si detector, placed 11 cm apart the Bi/Si target sample at 165° relative to the primary beam direction. The absolute uncertainties in the measured sputtering yields were estimated as in reference [17]. They essentially resulted from errors propagating in ion fluence expression (amounting to ~20%) and errors in the target sample areal densities (ranging only between 1% and 3%), and amount, at most, to ~25%. Finally, the AFM and XRD techniques (applied, respectively, at a 7° grazing incidence angle and in tapping mode) were used to investigate the surface topography and crystalline structure evolutions of the SHI irradiated Bi film surfaces.

3. Results, analyses and discussion

3.1. Sputtering yield, comparison to theory

Recorded RBS spectra for Bi/Si samples irradiated with incident 27.5 MeV $^{84}Kr^{15+}$ ions of fluences ranging between 8.9×10^{12} cm^{-2} and 1.35×10^{14} cm^{-2} are reported in Fig. 1, together with a reference spectrum for an un-irradiated sample. As observed in all such spectra, one can see that the initially deposited Bi film thickness significantly reduces upon SHI irradiation as ion fluence increases. One can also note the absence of any atomic interface mixing in the irradiated Bi/Si samples over the ion fluence range investigated. This observation is consistent with at least two previous results [22,23] for Bi/Si samples irradiated by SHI, suggesting that the effect of the latter on the target atomic mixing depends not only on the sensitivity of interface-forming materials to the electronic energy deposition but also on chemical driving forces that prevent inter-diffusion to occur in the thermal spike region. The RBS spectra for the irradiated samples were simulated by the RUMP computer code [24] in order to determine quantitatively the variation of the Bi sample thickness following SHI impacts. The areal density of the un-irradiated sample was estimated to be of $\sim(8.1 \pm 0.2) \times 10^{17}$ at/cm^2 corresponding to linear mean thickness, t, of ~289 ± 7 nm. However, as can be seen in Fig. 2, this initial mean value reduces linearly by ~4% up to 7% with increasing incident ion fluence. As proceeded in reference [17], the mean rate of removed Bi material

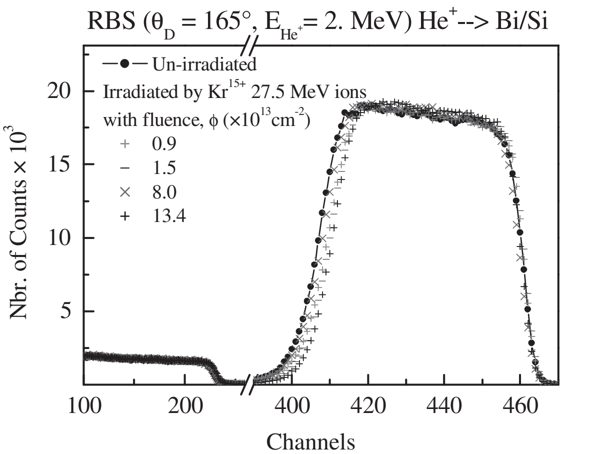

Fig. 1. RBS spectra for 2 MeV 4He$^+$ ions scattered at θ_{lab} = 165° off a 300 nm-thick Bi film deposited onto Si substrate following irradiation by 27.5 MeV $^{84}Kr^{15+}$ ions at different ion fluences.

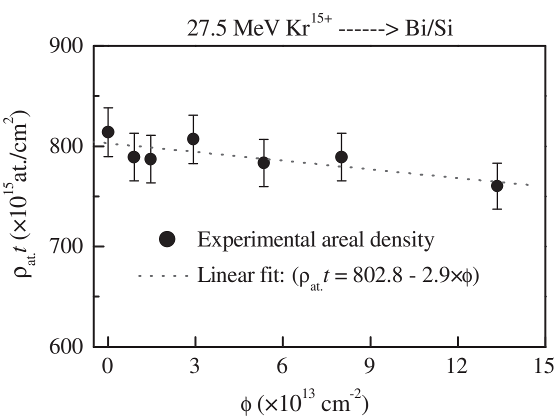

Fig. 2. Variation versus ion fluence of the Bi areal atomic density upon irradiation by 27.5 MeV $^{84}Kr^{15+}$ ions.

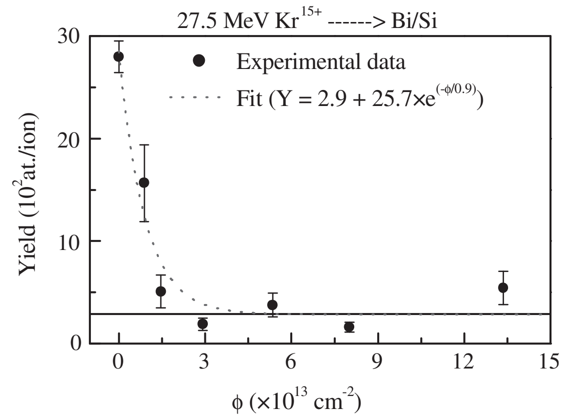

Fig. 3. Sputtering yield versus ion fluence for Bi thin films irradiated by 27.5 MeV $^{84}Kr^{15+}$ ions.

or mean sputtering yield, $\bar{Y}$, was directly determined from the fit-curve to the Bi areal density difference versus ion fluence, given by:

$$N_{Bi}(\phi) = \rho_{at.}t|_0 - \rho_{at.}t|_{irr.} = \bar{Y} \times \phi, \tag{1}$$

where $\rho_{at.}t|_0$ and $\rho_{at.}t|_{irr.}$ depict, respectively, Bi areal densities before and after ion irradiation, and $\rho_{at.}$ is the atomic density of the Bi film. The measured mean sputtering yield $\bar{Y}$ amounts to $\sim(2.9 \pm 0.9) \times 10^2$ at/ion. A similar enhanced sputtering yield of the same order of magnitude ($\bar{Y} \sim 200$ at/ion) has been reported recently [25] for Bi thin films irradiated by 120 MeV Au ions that was attributed to electronic collision effects ($S_e \approx 20$ keV/nm close to the expected threshold for strong surface effects to occur). The same hypothesis may be valid for the current experiment performed under similar conditions. It is supported by the fact that semimetals like-Bi are very sensitive to SHI irradiation effects inducing large sputtering yield and efficient surface damage [7–10], as will be detailed later in this section. The sputtering yield at each stage of SHI bombardment, determined from the slope, $\Delta N_{Bi}/\Delta\phi$, of the fit curve in Fig. 2, is depicted in Fig. 3 versus $^{84}Kr^{15+}$ ion fluence. The variation of $\Delta N_{Bi}/\Delta\phi$ versus ion fluence is well described by a decreasing exponential function [28] of the form

$$\frac{\Delta N_{Bi}}{\Delta\phi} = A + B \times \exp(-\phi/\phi_0) \tag{2}$$

where A, B and ϕ_0 are fit coefficients. One observes that the sputtering yield drastically decreases, first, below an ion fluence limit-value of $\sim 9.1 \times 10^{12}$ cm^{-2}, then, stands nearly constant ($\bar{Y} = A \approx (2.9 \pm 0.9) \times 10^2$ at/ion) over a saturation regime up to the highest ion fluence used ($\phi \approx 1.34 \times 10^{14}$ cm^{-2}). This behavior of the sputtering yield has been firstly observed by Andersen et al. [26] in the case of thin gold thin films (Au/C) irradiated by various 15 MeV ions (^{12}C, ^{14}N, ^{16}O, ^{19}F, ^{35}Cl, ^{79}Br). It was interpreted to be caused by two competing processes: (i) a rapid degradation of the Au films due to the same ionization mechanism as that occurring with fission fragment tracks in thin discontinuous metal films followed by (ii) a stabilization of the target erosion due to ionization-induced cracking of hydrocarbon. In an other hand, this trend (but with yields of lower order of magnitude) is also similar to that we have pointed out recently for Bi/Si thin films irradiated by 60 and 120 keV Ar$^+$ ions [17,18] (see Fig. 8 of Ref. [17]). Such a close dependence of the sputtering yield on ion fluence was ascribed to the Bi target material nature and to the changes induced by ion irradiation in its surface topography and crystalline structure at a microscopic level [17,27–29]. In the case of tens keV Ar$^+$ incident ions, where nuclear and electronic energy losses amount to comparable magnitudes, we assumed a rather complex interplay between elastic and inelastic collision processes for interpreting the observed surface effects induced in Bi thin films [17,18], although mechanisms involving mainly elastic collisions could be dominating.

Estimating the sputtering yields in the current case for a Bi target bombarded by 27.5 MeV ^{84}Kr ions from Sigmund's sputtering theory [19] based on the binary collision approximation and assuming the formation of linear elastic collision cascades, one obtains $\bar{Y} \sim 5.9$ at/ion; i.e., a value much lower than the above experimental $\bar{Y}$ -value. An additional contribution due to elastic collision spikes when both the projectile and target are heavy is neglected here since the sputtering yield estimated by the Sigmund–Claussen thermal spike model [30] amounts to only $\sim$0.65 at/ion. Besides, a possible enhancement of the sputtering yield due to potential energy for highly charged ions is ruled out in the current case because the $^{84}Kr^{15+}$ incident ions are in the equilibrium charge state corresponding to the most probable charge state distribution [5,6,26,31], i.e., of the order of the effective charge defined by electronic energy loss predictions. Therefore, one is led to conclude that the observed high sputtering yield and other observed Bi surface effects undergone by the Bi target under irradiation by 27.5 MeV $^{84}Kr^{15+}$ ions are conceivably driven mainly by inelastic electronic collision energy loss effects. However, the predominance of these processes (inelastic ion/atom collisions, atomic displacements) over elastic nuclear collision effects may be considered as not clearly enough established here in the absence of an investigation of the energy dependence of the Bi sputtering yield.

3.2. AFM and XRD analyses

The AFM scans of the Bi film surfaces performed before and after ion irradiation with two largely different ion fluences of 5.3×10^{13} cm^{-2} and 1.34×10^{14} cm^{-2} have led us to the resulting images in 3D-representation reported in Fig. 4. As expected for Bi thin films deposited by conventional techniques [17,21], the un-irradiated Bi sample surface appears to be composed of two types of grain structures: (i) small grains of ~50–80 nm width and less than 100 nm height and (ii) much larger granular structures of ~200–500 nm width and ~100–150 nm-height in lower proportion (see Fig. 4a).

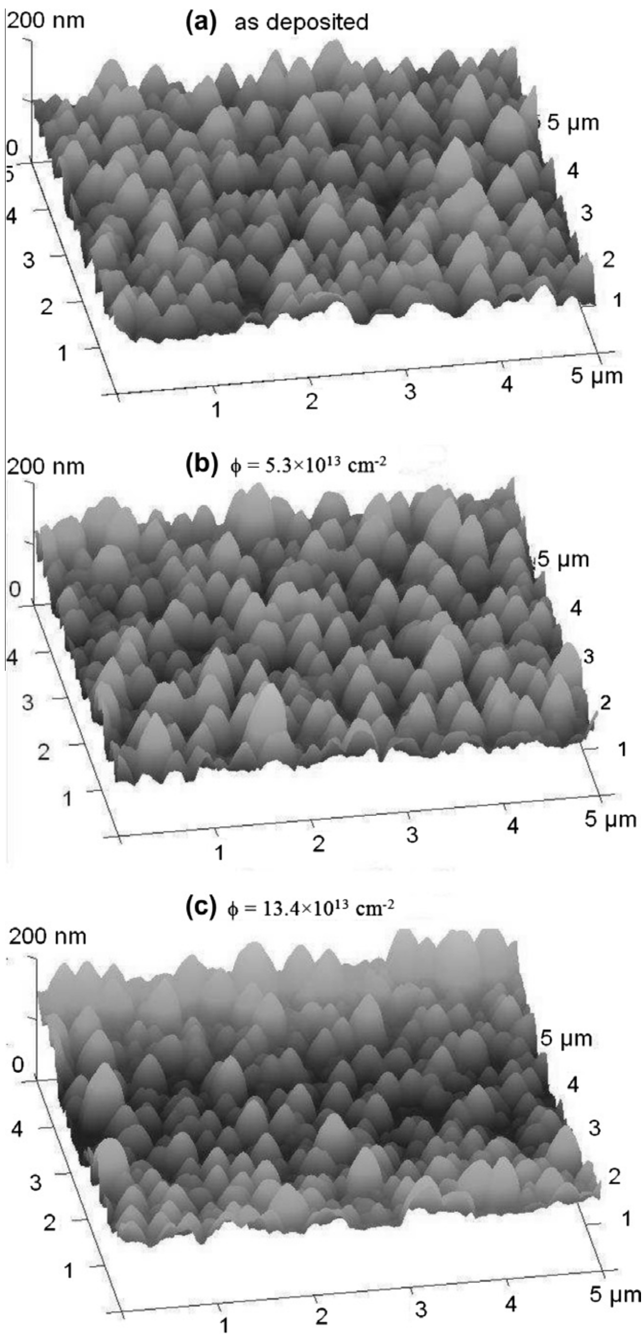

Fig. 4. AFM images (in 3D) of Bi film surfaces: (a) a Bi/Si un-irradiated sample, (b and c) Bi/Si samples irradiated by 27.5 MeV $^{84}Kr^{15+}$ ions of fluences $\phi \sim 5.3 \times 10^{13}$ cm^{-2} and 1.34×10^{14} cm^{-2}, respectively.

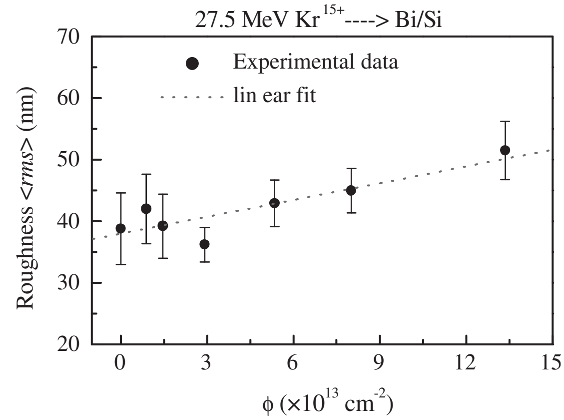

Fig. 5. Variation of Bi surface roughness versus ion fluence upon irradiation by 27.5 MeV $^{84}Kr^{15+}$ ions, derived by AFM analysis.

Upon irradiation, one observes an increase of the grain sizes and a decrease of the number of granular structures versus ion fluence (see Fig. 4b and c). The *rms* surface roughness, defined as the mean standard deviation of the grain heights and granular structures observed on a-1 µm^2 area of the scanned whole surface, was also determined experimentally by AFM treatment. The results of Bi surface roughness measurements in function of incident ion fluence are depicted in Fig. 5. The obtained experimental data thus exhibit a linear increase of the Bi surface roughness with increasing ion fluence: as can be seen, the *rms* parameter evolves from ~38.8 nm before irradiation up to 51.5 nm upon SHI bombardment at the largest fluence used ($\phi \approx 1.34 \times 10^{14}$ cm^{-2}). The substantial increase in the Bi surface roughness is expected to be due to a high electronic energy density deposition by the $^{84}Kr^{15+}$ incident ions. Then, atomic displacements and defect creations are induced through the irradiated Bi film surface [18,32,33], giving rise to the grain growth clearly shown by the AFM images. The microstructures of both the pristine and irradiated Bi film-surfaces were analyzed by recording corresponding XRD patterns reported in Fig. 6. One can observe, first in Fig. 6a, that the un-irradiated Bi film has a polycrystalline structure with two (003) and (006) predominant peaks and other various orientations, i.e., (012), (104), (110), (202), (024), (205), (303) and (009). The observed preferential orientation of as-deposited samples is due to the growth under low evaporation rate of crystallites perpendicular to the substrate surface as expected for Bi thin films deposited by evaporation technique [17,21]. Then, following SHI irradiation, the peak intensities of both the (003) orientation and its (006) second and (009) third-order reflections increase with increasing ion fluence. This observation is consistent with the Bi grain size enhancement revealed by the AFM analysis. The (003) crystallite sizes (D) were determined using the well-known Sherrer X-ray diffraction formula [34]:

$$D_{003} = \frac{0.9\lambda}{\beta \cos\theta} \tag{3}$$

where λ = 1.5406 Å is the Cu-K$_\alpha$ line wavelength, θ the Bragg diffraction angle and β the diffraction peak width (FWHM) expressed in radians. The obtained results are reported in Fig. 7. While the initial D_{003}-value amounts to ~76.1 nm, upon SHI irradiation it sharply increases with increasing ion fluence, reaching a maximum value of ~87 nm for $\phi = 5.3 \times 10^{13}$ cm^{-2}, then, remains nearly constant as ϕ increases beyond this value. Examining further the recorded XRD patterns of Fig. 6, one can also observe an increased shift of the peak position towards higher diffraction angles with increasing ion fluence. This peak shifting might be due to the modification of

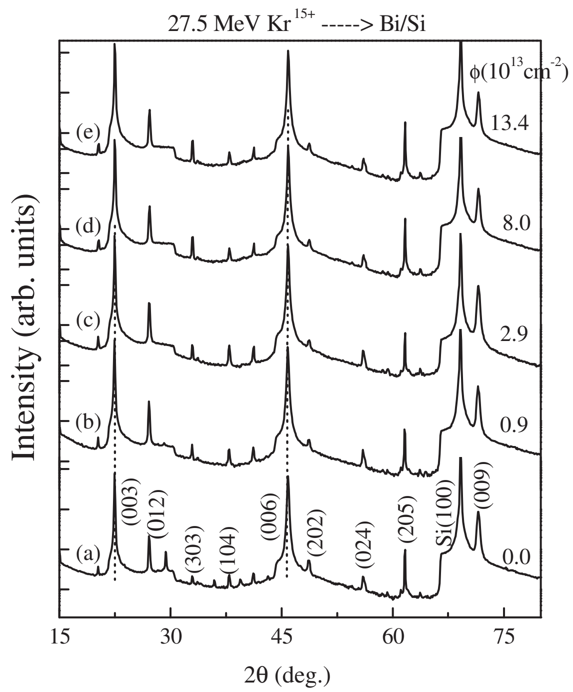

Fig. 6. X-ray diffraction patterns: (a) for a Bi/Si un-irradiated sample; (b–f) for Bi/Si samples irradiated by 27.5 MeV $^{84}Kr^{15+}$ ions at fluences of 8.9×10^{12} cm^{-2}, 2.9×10^{13} cm^{-2}, 5.3×10^{13} cm^{-2}, 8.0×10^{13} cm^{-2} and 1.34×10^{14} cm^{-2}, respectively.

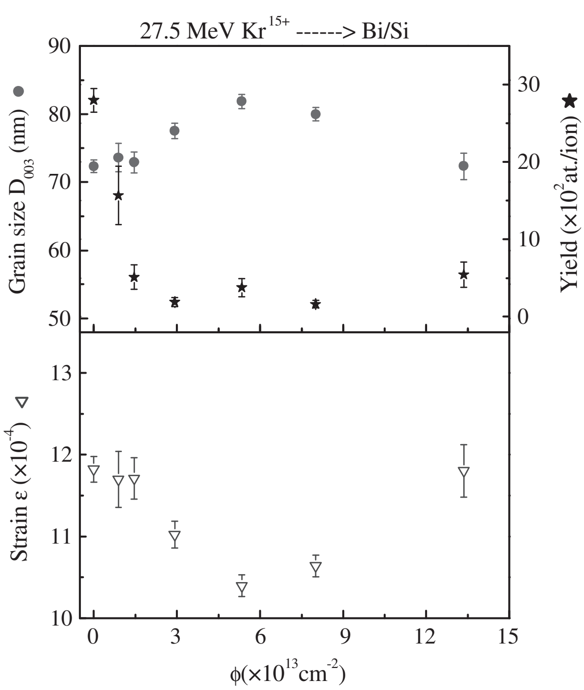

Fig. 7. Grain size and lattice strain variations versus ion fluence upon irradiation of Bi by 27.5 MeV $^{84}Kr^{15+}$ ions, derived by XRD analysis (see Eqs. (3) and (4)). The measured sputtering yield is also represented.

the lattice strain due to compressive stress induced point defects with increasing the total electronic energy deposited by incident ions per target mass unit [27,35,36], i.e., as the Kr^{15+} ion dose, $d \sim S_e \times \phi$, increases. The lattice strain towards the (003) orientation peak was calculated by the relation [37]

$$\varepsilon_{003} = \frac{\beta}{4\tan\theta} \tag{4}$$

The obtained results are also reported in Fig. 7. As can be seen, the $\varepsilon(\phi)$ function exhibits a reverse trend relative to the grain growth, starting to decrease down to a minimum for $\phi = 5.3 \times 1013$ cm-2 (corresponding to maximum target roughness), then increasing (while the Bi roughness decreases) beyond this ion fluence value. Note that the variation of the $\varepsilon(\phi)$ function also bears close similarities with that shown by the measured sputtering yield also depicted for comparison in Fig. 7. Therefore, it turns out that both the grain size and the compressive strain behaviors versus ion fluence seem to be closely correlated to that of the experimental sputtering yield. Indeed, practically reverse variations of the (Y, ε) and D_{003} functions of ϕ are observed with marked (reverse) nearly saturated regimes. These correlated behaviors likely link to Bi material specific intrinsic properties that suffer drastic changes under ion irradiation caused by deposited large electronic energy density confined in a very small sample volume. Consistently with previous reports [4,7–11,15,38], the SHI irradiated Bi material then likely undergoes strong modifications connected to its heat transport proprieties. Indeed, following their interaction with the sample surface, the incident SHI lose kinetic energy within a nanometer-sized volume close to the sample surface, which probably gives rise to a tiny, highly unstable matter region around the ion path submitted to large electronic excitation [9,10]. The subsequent transfer of the latter to the material lattice atoms may cause a strong local heating [39] of this excited zone that could even be at least partly molten. Note that a recent numerical study [40] based on molecular dynamics simulation confirms the predominance of thermal energy transfer mechanisms over coulomb interaction effects under irradiation of materials by swift heavy ions. However, for electronic stopping power values lower than the predicted threshold ($S_e^{th} \sim 24$ keV/nm in Bi, Ref. [8]) as is the case for incident 27.5 MeV $^{84}Kr^{15+}$ ions losing only ~8.08 keV/nm in Bi, the material heating cannot reach its melting point but is sufficient for generating the observed Bi thin film surface modifications, e.g., grain growth, compressive strain induced defects, surface roughening and sputtering. These observed moderate Bi surface effects induced by irradiation with 27.5 Kr^{15+} ions are quite similar to those observed previously on similar films bombarded by 120 MeV Au ions [25] as well as by keV Ar^{+} ions [17,18]. The only difference between the two sets of heavy ion irradiation effects seems to rely only on differences in the deposited energy densities. Indeed, it must be noted, e.g., that the reorientation of the main crystallographic direction of a polycrystalline sample under ion irradiation is not restricted to electronic energy loss effects as has been observed earlier [41] on polycrystalline Cu bombarded with 40 keV Ni ions under elastic nuclear stopping power conditions.

4. Summary, further discussion and conclusion

In this work, we have investigated the sputtering and surface topography modifications suffered by Bi thin films irradiated by 27.5 MeV $^{84}Kr^{15+}$ ions in the equilibrium charge state over the range of incident ion fluences $\phi = 10^{12}$–10^{14} cm^{-2}. In these SHI irradiation conditions, one expects only moderate Bi surface effects to occur below the target electronic stopping power threshold ($S_e^{th} \sim 24$ keV/nm) required for the material melting and the formation of extended latent tracks. Indeed, the irradiated Bi films exhibit increasing surface grain growth and roughening, clearly pointed out by the performed AFM and XRD analyses. More precisely, larger grains oriented to the preferred (003) trigonal crystalline structure and a linear increase of the determined Bi mean surface roughness, D_{003}, with increasing ϕ are observed. As a result, substantially enhanced Bi sputtering occurs under SHI impacts, reflected by a linear decrease of the areal density with increasing ion fluence and evidenced by RBS spectrometry. Finally, a close correlation is pointed out between the variations with ion fluence of several Bi surface effects: (i) the measured Bi sputtering yield decreasing towards a – steady state regime as ϕ increases, (ii) the observed grain growth on the irradiated Bi sample surface and (iii) the increasing crystalline alignment towards the 003 crystalline structure that would reflect the channeling of incident $^{84}Kr^{15+}$ ions. These observations are consistent with the fact that Sigmund's linear collision cascade theory [19], valid for an atomically flat target material surface, is unable to account for the measured absolute Bi sputtering yield. Furthermore, as we have seen, the calculation by Sigmund – Claussen model [30] considering nonlinear nuclear cascades fully underestimates the measured sputtering yield, although a high *Y*-value is expected regarding the low sublimation energy of Bi. The observed Bi surface effects under irradiation by 27.5 MeV $^{84}Kr^{15+}$ ions within the electronic stopping power regime show large similarities with our recently reported Bi surface effects induced by keV Ar^+ ions [17,18] within the Bi nuclear stopping power regime. Noteworthy, even in the latter experiments the sputtering yield data were not accounted for satisfactorily by Sigmund's linear cascade theory but by the Bodhansky and Yamamura et al. semi-empirical models [42,43] involving both nuclear and electronic energy loss interaction processes, and valid only within the keV ion energy range. Therefore, as stated in [17,18], a complex interplay between different interaction mechanisms related to elastic nuclear collisions and inelastic electronic collisions seems to cause the resulting observed Bi surface effects under keV Ar^+ ions. In the current case of 27.5 MeV Kr^{15+} ions incident on Bi, however, considering mainly the large magnitude of the measured sputtering yield not reproduced neither by the linear nor by the non linear nuclear collision cascade theories, one is led to assume that the ion–solid interaction mechanisms due to inelastic electronic collisions are likely predominant. This is consistent with the fact that for incident swift $^{84}Kr^{15+}$ ions, the Bi electronic stopping power (increasing as $\sim E^{1/2}$) considerably dominates the target nuclear stopping power (decreasing as E^{-1}, i.e., $S_e \sim 8.08$ keV/nm >> S_n - ~ 0.18 keV/nm). Observing similar Bi surface effects as in the current experiment upon irradiation by swift Au ions, the authors of reference [25] also arrived at the same conclusion. This interpretation (predominance of electronic collision interaction mechanisms over nuclear collision ones in materials SHI irradiation) is, besides, supported by several other recent studies [44–46] (and references therein) conducted by different groups in the higher part of the target electronic stopping power regime. Such studies have investigated SHI irradiation-induced effects on: (i) the properties of semiconductor materials [44] pointing out the annealing (due to electronic collision processes) of defects (vacancies, interstitials) induced by elastic nuclear collisions, and (ii) Bi compound materials interpreting the observed strong induced surface effects by invoking the thermal spike model [45,46]. Nevertheless, in order to definitely confirm this assumption and clarify whether or not electronic energy loss effects completely dominate over elastic nuclear collision processes, additional measurements of the energy dependence of the Bi sputtering yield within the (10–50) MeV energy range of the $^{84}Kr^{15+}$ incident ions is highly desirable. Furthermore, experiments where swift Bi ions or Bi clusters are used as projectiles for irradiating Bi thin films within the lower part of the Bi electronic stopping power regime would be surely of great interest for a complete elucidation of ion–solid interaction mechanisms put into play. Then, one would be concerned by bismuth self-sputtering, which would enjoyably allow avoiding the contamination of the irradiated Bi samples by implantation of incident SHI of different nature than the scanned target.

Acknowledgements

The authors are grateful to the National Research Foundation (NRF) of South Africa and to the Algerian Atomic Energy Commission (COMENA) for providing financial support for this work. They also would like to thank Professor M. Maaza for his precious assistance, Dr. M. Nkosi for AFM analysis and Dr L. Conradie for beam time irradiation at the Cyclotron accelerator of iThemba Labs, Cape Town (South Africa).

References

[1] R. Behrisch, K. Wittmaack (Eds.), Sputtering by Particle Bombardment, Topics in Applied Physics, vol. 64, Springer, Berlin, 1991.
[2] V.S. Smentkowski, Trends in sputtering, Prog. Surf. Sci. 64 (2000) 1.
[3] R. Behrisch, W. Eckstein (Eds.), Sputtering by Particle Bombardment, Topics in Appl. Phys., vol. 110, Springer-Verlag, 2007.
[4] W. Assmann, M. Toulemonde, C. Trautmann, Sputtering by Particle Bombardment, Topics in Appl. Phys. 110 (2007) 401.
[5] H.D. Mieskes, W. Assmann, M. Brodale, M. Dobler, H. Glückler, P. Hartung, P. Stenzel, Nucl. Instrum. Methods Phys. Res. B 146 (1998) 162.
[6] H.D. Mieskes, W. Assmann, F. Grüner, Phys. Rev. B 67 (2003) 155414.
[7] C. Dufour, A. Audouard, F. Beuneu, J. Dural, J.P. Girard, A. Hairie, M. Levalois, E. Paumier, M. Toulemonde, J. Phys. Condens. Matter 5 (1993) 4573.
[8] Z.G. Wang, C. Dufour, E. Paumier, M. Toulemoude, J. Phys.: Condens. Matter 6 (1994) 6733.
[9] M. Toulemonde, C. Dufour, E. Paumier, Acta Phys. Pol., A 109 (3) (2006) 311.
[10] C. Dufour, F. Beuneu, E. Paumier, M. Toulemonde, Europhys. Lett. 45 (5) (1999) 585.
[11] R.L. Fleischer, P.B. Price, R.M. Walker, Nuclear Tracks in Solids: Principles and Applications, University of California Press, Berkeley, 1975.
[12] E.M. Bringa, R.E. Johnson, Nucl. Instrum. Methods Phys. Res. B 143 (1998) 513; E.M. Bringa, R.E. Johnson, M. Jakas, Phys. Rev. B 60 (22) (1999) 15107; E.M. Bringa, M. Jakas, R.E. Johnson, Nucl. Instrum. Methods Phys. Res. B 164-165 (2000) 762.
[13] W.M. Arnoldbik, N. Tomozeiu, F.H.P.M. Habraken, Nucl. Instrum. Methods Phys. Res. B 203 (2003) 151.
[14] D.K. Avasthi, S. Ghosh, S.K. Srivastava, W. Assmann, Nucl. Instrum. Methods Phys. Res. B 219-220 (2004) 328.
[15] M. Kumar, S.A. Khan, F. Singh, A. Tripathi, D.K. Avasthi, A.C. Pandey, Nucl. Instrum. Methods Phys. Res. B 256 (2007) 328.
[16] M. Kumar, P. Rajput, S.A. Khan, D.K. Avasthi, A.C. Pandey, Appl. Surf. Sci. 256 (2010) 2199.
[17] S. Mammeri, S. Ouichaoui, H. Ammi, R. Zemih, Nucl. Instrum. Methods Phys. Res. B 268 (2010) 140.
[18] S. Mammeri, S. Ouichaoui, H. Ammi, H. Hammoudi, C.A. Pineda-Vargas, Nucl. Instrum. Methods Phys. Res. B 269 (2011) 909.
[19] P. Sigmund, Phys. Rev. 184 (1969) 38.
[20] J.F. Ziegler, J.P. Biersack, U. Littmark, The Stopping and Range of Ions in Solids, Pergamon, New York, 1985. TRIM/SRIM computer code, available at http://www.srim.org..
[21] Latha. Kumari, Shih.-Jie. Lin, Jin.-Han. Lin, Yuan.-Ron. Ma, Ping.-Chung. Lee, Yung. Liou, Appl. Surf. Sci. 253 (2007) 5931.
[22] R. Nakatani, R. Taniguchi, Y. Chimi, N. Ishikawa, M. Fukuzumi, Y. Kato, H. Tsuchida, N. Matsunami, A. Iwase, Nucl. Instrum. Methods Phys. Res. B 230 (2005) 234.
[23] H. Paulus, T. Bolse, W. Bolse, Nucl. Instrum. Methods Phys. Res. B 245 (2006) 117.
[24] L.R. Doolittle, Nucl. Instr. and Meth. in Phys. Res. B 9 (1985) 344. RUMP computer code available at http://www.genplot.com.
[25] A. Gupta, R.S. Chauhan, D.C. Agarwal, S. Kumar, S.A. Khan, A. Tripathi, D. Kabiraj, S. Mohapatra, T. Som, D.K. Avasthi, J. Phys. D: Appl. Phys. 41 (2008) 215306.
[26] H.H. Andersen, H. Knudsen, P. Møller Petersen, J. Appl. Phys. 49 (1978) 5638.
[27] J.W. Burnett, M.J. Pellin, W.F. Calaway, D.M. Gruen, J.T. Yates, Phys. Rev. Lett. 63 (1989) 562.
[28] A. Mutzke, W. Eckstein, Nucl. Instrum. Methods. Phys. Res. B 266 (2008) 872.
[29] D. Datta, S.R. Bhattacharyya, Appl. Surf. Sci. 255 (2008) 2075.
[30] P. Sigmund, C. Claussen, J. Appl. Phys. 52 (1981) 990.
[31] T. Schenkel, M.A. Briere, H. Schmidt-Böcking, K. Bethge, D.H. Schneider, Phys. Rev. Lett. 78 (1997) 2481.
[32] N.K. Kachhap, S.K. Dubey, R.L. Dubey, A.D. Yadav, D. Kanjilal, S.K. Deshpande, Surf. Coat. Technol. 203 (2009) 2422.
[33] H.D. Mieskes, W. Assmann, F. Grüner, Phys. Rev. B 67 (2003) 155414.
[34] B.D. Cullity, S.R. Stock, Elements of X-ray Diffraction, 3rd edition., Prentice Hall, USA, 2001.
[35] S. Banerjee, A. Kumar, Nucl. Instrum. Methods Phys. Res. B 268 (2010) 2683.
[36] P. Mallick, C. Rath, J. Prakash, D.K. Mishra, R.J. Choudhary, D.M. Phase, A. Tripathi, D.K. Avasthi, D. Kanjilal, N.C. Mishra, Nucl. Instrum. Methods Phys. Res. B 268 (2010) 1613.
[37] T.H. de Keijser, J.I. Langford, E.J. Mittemeijer, A.B.P. Vogels, J. Appl. Cryst. 15 (1982) 308.

[38] S. Ghosh, A. Ingale, T. Som, D. Kabiraj, A. Tripathi, S. Mishra, S. Zhang, X. Hong, D.K. Avasthi, Solid State Commun. 120 (2001) 445.
[39] A.S. El-Said, R.A. Wilhelm, R. Heller, S. Facsko, C. Trautmann, F. Aumayr, Nucl. Instrum. Methods. Phys. Res. B 269 (2011) 1234.
[40] P. Baril, L.J. Lewis, S. Roorda, Eur. Phys. J. B 71 (2009) 27.
[41] G.H. Vanwyk, H.J. Smith, Radiat. Eff. 38 (1978) 245.
[42] J. Bodhansky, Nucl. Instrum. Methods Phys. Res. B 2 (1984) 587.
[43] Y. Yamamura, H. Tawara, At. Data Nucl. Data Tables 62 (1996) 149.
[44] S. Kumar, Y.S. Katharria, Y. Batra, D. Kanjilal, J. Phys. D: Appl. Phys. 40 (2007) 6892.
[45] R.R. Ahire, Abhay A. Sagade, S.D. Chavhan, V. Huse, Y.G. Gudage, F. Singh, D.K. Avasthi, D.M. Phase, R. Sharma, Curr. Appl. Phys. 9 (2009) 374.
[46] A. Gupta, D.C. Agarwal, S.A. Khan, A. Tripathi, D. Kabiraj, S. Mohapatra, T. Som, D.K. Avasthi, R.S. Chauhan, Surf. Coat. Technol. 203 (2009) 2399.